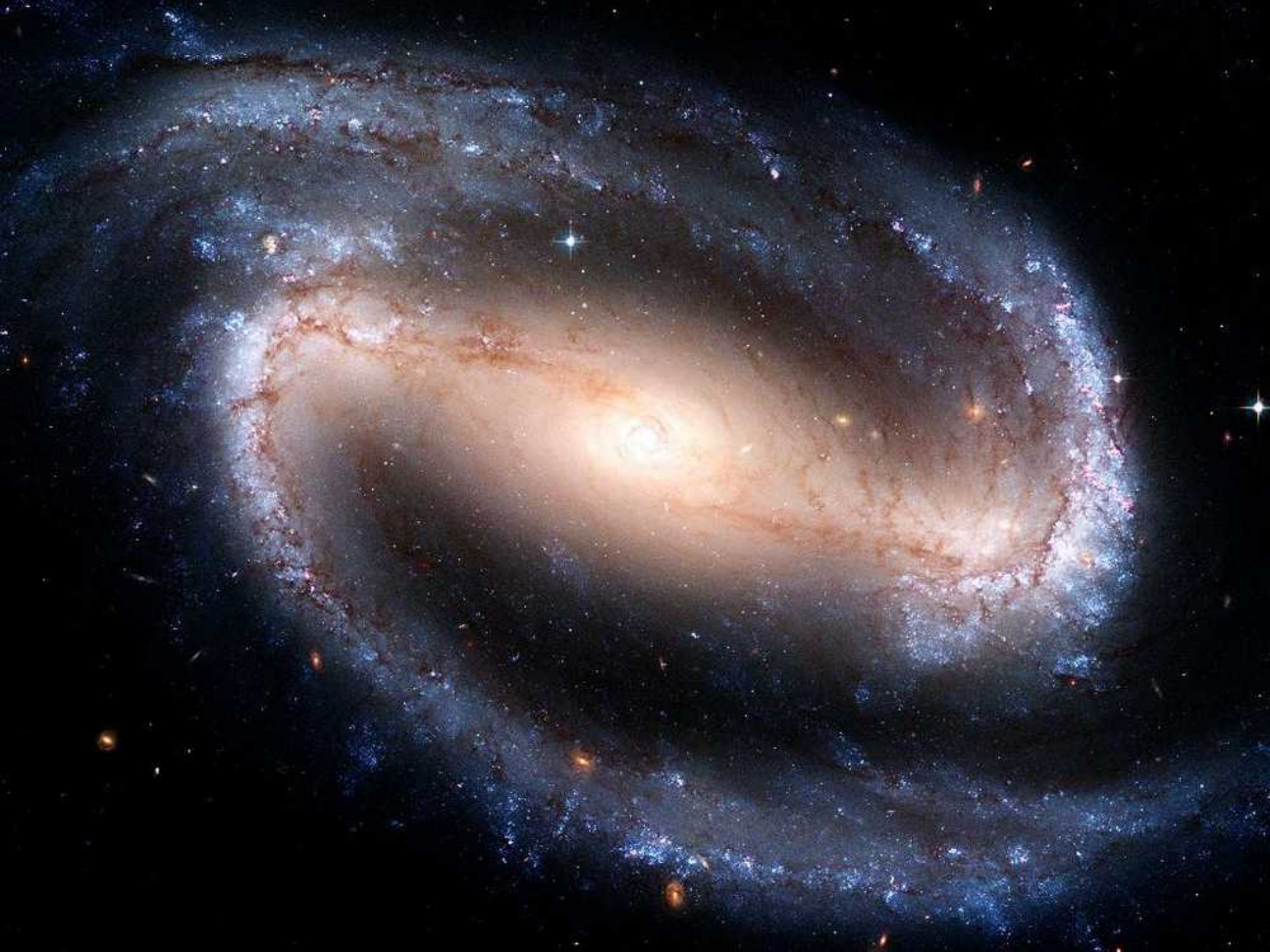


A barred spiral galaxy is shown, viewed from an angle. The central region is bright and yellowish, indicating a high concentration of stars. The spiral arms are dark, with numerous bright blue spots scattered throughout, representing regions of active star formation. The overall color palette is dominated by deep blues and oranges, with the central core being the brightest.

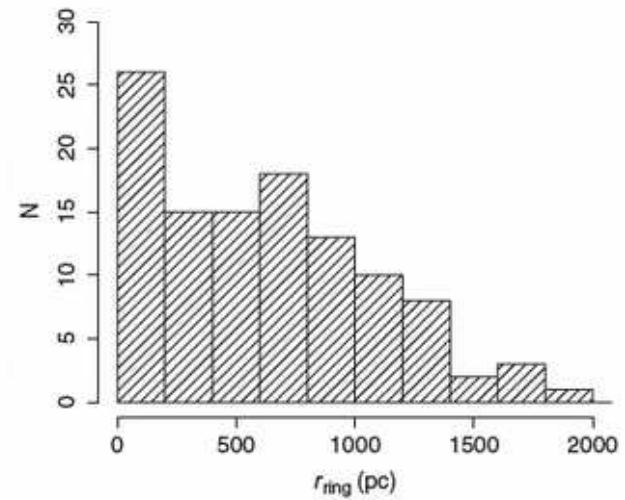
Star Formation in the Nuclear Region of Barred Galaxies

Woo-Young Seo & Woong-Tae Kim
Seoul National University, Korea



Observations

- Nuclear rings in barred galaxies are sites of intense star formation.
- Size of the nuclear rings varies from galaxy to galaxy (50pc ~ 2 kpc).
- The star formation rate (SFR) in the nuclear ring also differs fr



(Comeron et al. 2010)

Observations

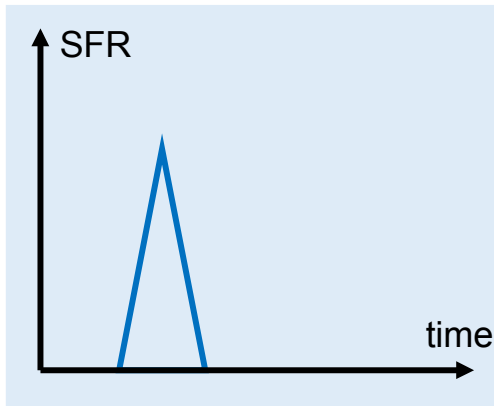
- Nuclear rings are sites of intense star formation

NGC (1)	Morph. Type (2)	ϵ_{Ring} (3)	PA_{Ring} (deg) (4)	R_{Ring} (arcsec) (5)	R_{Ring} (kpc) (6)	PA_{Disk} (deg) (7)	PA_{bar} (deg) (8)	SFR ($M_{\odot} \text{ yr}^{-1}$) (9)
278.....	SAB(rs)b	0.06	120	4.4 × 4.1	0.2 × 0.2	...	No bar	0.5
473.....	SAB(r)0/a	0.37	160	12.2 × 6.9	1.7 × 1.0	153	164	2.2
613.....	SB(rs)bc	0.3	122	5.1 × 2.6	0.4 × 0.2	120	120	2.2
1300.....	(R)SB(s)bc	0.25	135	4.1 × 3.1	0.3 × 0.2	106	102	0.2
1343.....	SAB(s)b	0.25	60	8.8 × 6.6	1.2 × 0.9	80	82	6.8
1530.....	SB(rs)b	0.35	25	6.8 × 4.9	1.2 × 0.8	8	122	3.8
4303.....	SAB(rs)bc	0.14	88	3.3 × 2.8	0.2 × 0.2	...	10	1.4
4314.....	SB(rs)a	0.10	135	6.6 × 5.9	0.3 × 0.3	...	135	0.1
4321.....	SAB(s)bc	0.12	170	8.8 × 7.0	0.7 × 0.6	30	153	...
5248.....	(R)SB(rs)bc	0.3	115	6.6 × 4.6	0.7 × 0.5	110	137	4.2
5728.....	(R1)SAB(r)a	0.4	125	5.3 × 3.2	1.1 × 0.6	...	33	4.0
5905.....	SB(r)b	0.2	141	1.6 × 1.5	0.3 × 0.3	135	25	2.6
5945.....	SB(rs)ab	0.1	105	3.5 × 3.2	1.2 × 1.1	105	10	4.4
5953.....	SAa	0.1	192	6.1 × 5.5	1.0 × 0.9	169	no bar	9.9
6503.....	SA(s)cd	0.65	121	38.5 × 13.4	1.1 × 0.4	123	no bar	1.5
6951.....	SAB(rs)bc	0.2	146	4.6 × 3.7	0.5 × 0.4	170	85	1.4
7217.....	(R)SA(r)ab	0.20	89	11 × 8.8	0.8 × 0.7	95	no bar	0.6
IC 1438.....	SAB(r)a	0.10	130	3.3 × 3.0	0.5 × 0.5	...	124	1.3
7469.....	SAB (rs)a	0.09	38	1.6 × 1.5	0.5 × 0.5	135	56	...
7570.....	SBa	0.05	135	4.4 × 4.2	1.3 × 1.3	30	30	1.4
7716.....	SAB(r)b	0.2	30	6.3 × 4.2	1.0 × 0.7	35	34	3.2
7742.....	SA(r)b	0.05	133	9.9 × 9.4	1.0 × 1.0	...	no bar	4.3

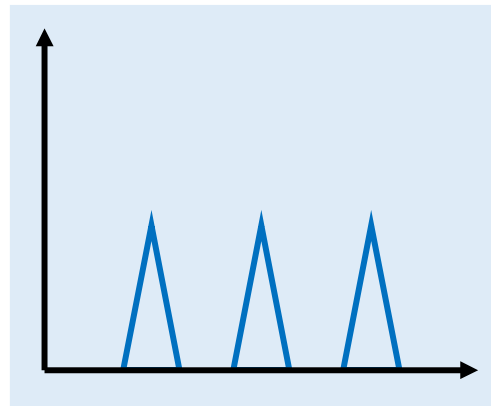
(Mazzuca et al. 2008)

- The star formation rate (SFR) in the nuclear ring also differs from the global SFR

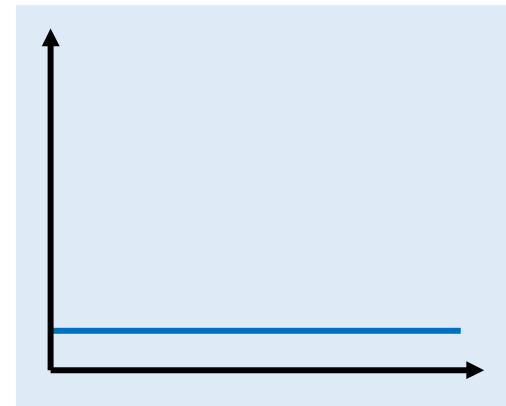
Observations



Single Burst Model



Multiple Bursts Model

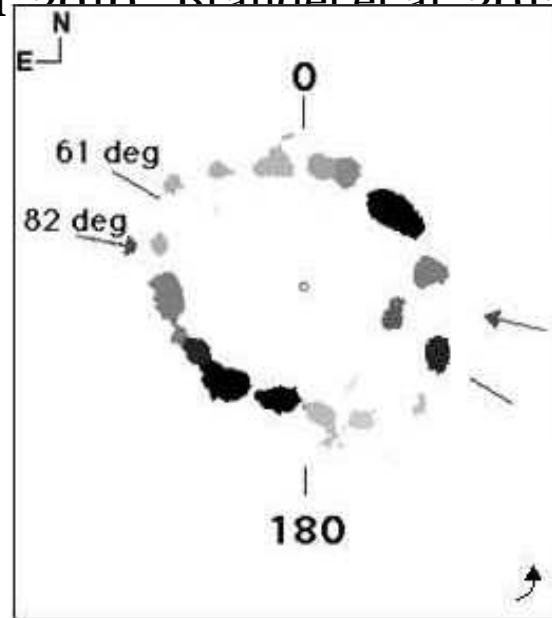


Continuous Model

- Continuous SF
 - van der Laan et al. (2013) found that the circumnuclear ring in NGC 6951 has been forming stars for recent ~ 1 Gyr.
- Multiple-burst SF
 - Using stellar population synthesis models Allard et al. (2006) estimated that M100(NGC 4321) shows multiple-burst type SF.
 - Sarzi et al. (2007) showed two galaxies (NGC4314 and NGC 7217) also have experienced multiple-burst SF using the same method.

Observations

- Locations of star formation
 - Some galaxies show an azimuthal age gradient.
 - Some galaxies do not show a noticeable age gradient.
- (Mazzuca et al. 2008, Ryder et al. 2010, Brandel et al. 2012)



NGC 1343 (Mazzuca et al. 2008)

Previous Simulations

- Hydrodynamic simulations
 - Athanassoula 1992; Maciejewski et al. 2002; Maciejewski 2004; Regan & Teuben 2003,2004
 - Englmaier & Gerhard 1997; Patsis & Athanassoula 2000; Ann & Lee 2000; Ann & Thakur 2005; Thakur et al. 2009
- N-Body (+SPH) simulations
 - Bournaud et al. 2005; Martinez-Valpuesta 2006; Berentzen et al. 2007; Manos et al. 2010; Minchev et al. 2012; Athanassoula 2012; Roca-Fabrega et al. 2013; Kwak et al. 2017

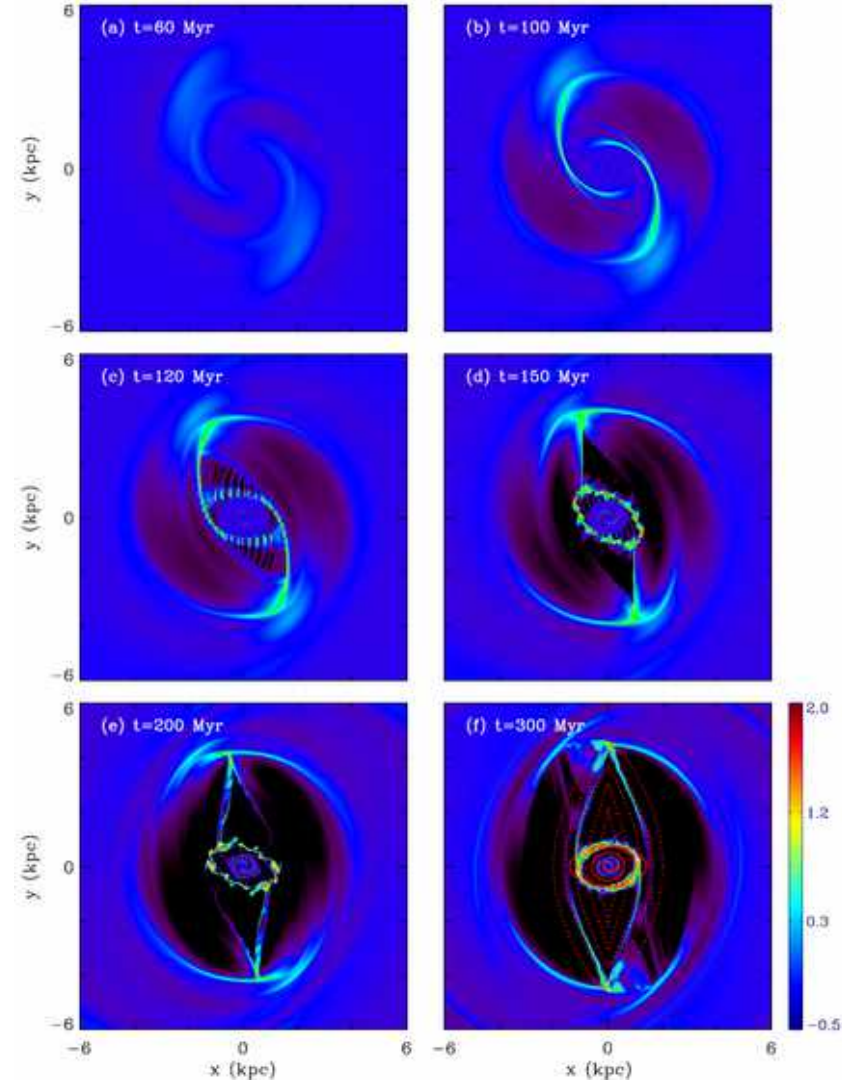
2D simulations

- Two dimensional cylindrical, non-uniform radial grid code, CMHOG2
- The gaseous disk is assumed to be isothermal and infinitesimally thin.
- The stars and dark matter are represented by a static gravitational potentials.
 - Stellar bar potential is modeled by a Ferrers (1877) prolate.
 - Semi-major / minor axes : 5 kpc / 2 kpc
 - Pattern speed : 33 km/s/kpc

Ring Formation

(Kim et al. 2012)

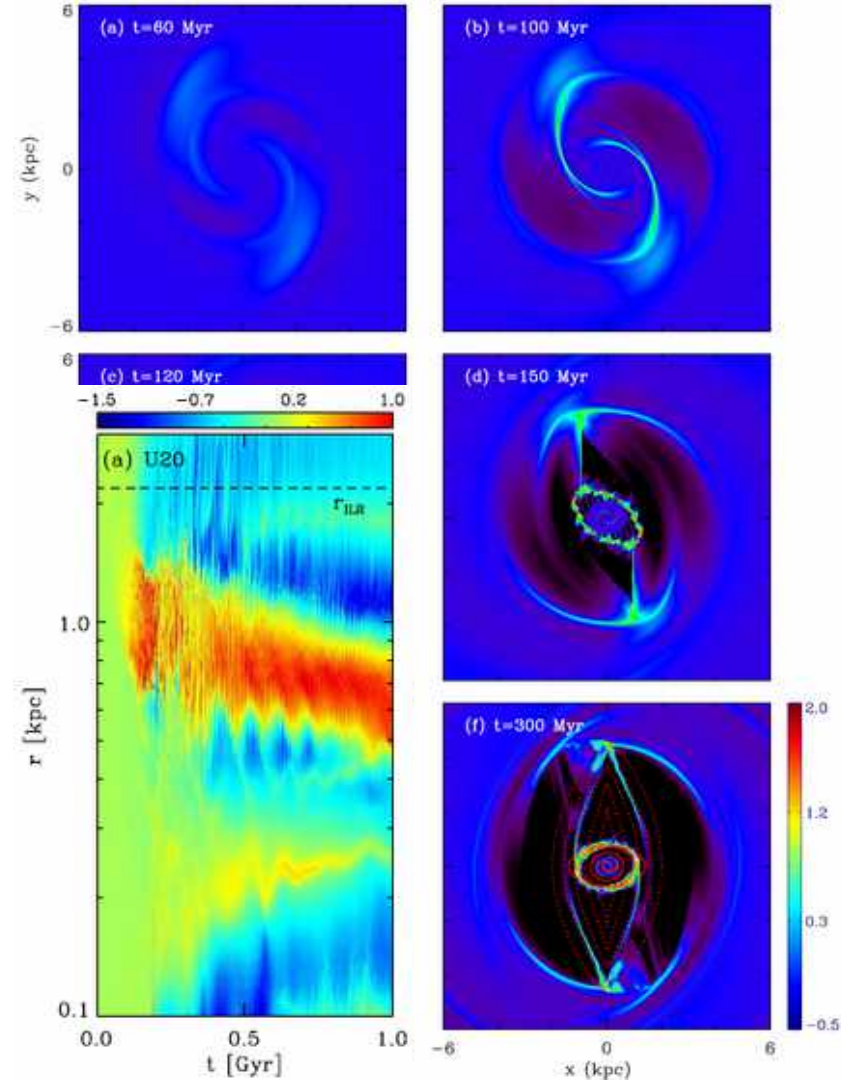
- Off-axis shocks are produced by growth of a non-axisymmetric bar potential.
- Gas loses its angular momentum when it passes through dust lanes and moves inward.
- The nuclear ring forms in the position where the centrifugal force balances the external gravity.
- In the static bar potential models, the nuclear rings shrink in radius with time because of an addition of gas with lower angular momentum.



Ring Formation

(Kim et al. 2012)

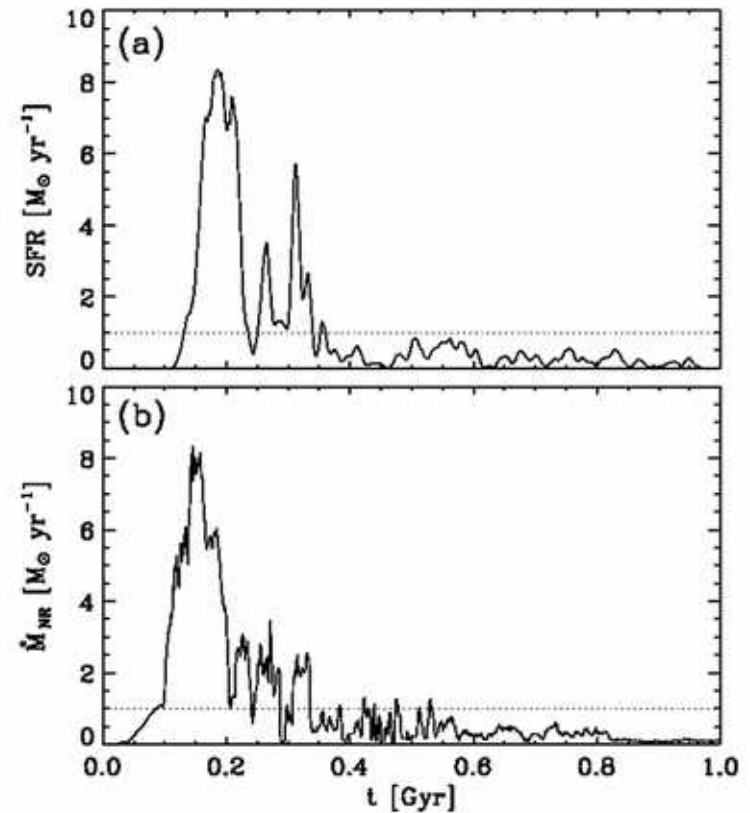
- Off-axis shocks are produced by growth of a non-axisymmetric bar potential.
- Gas loses its angular momentum when it passes through dust lanes and moves inward.
- The nuclear ring forms in the position where the centrifugal force balances the external gravity.
- In the static bar potential models, the nuclear rings shrink in radius with time because of an addition of gas with lower angular momentum.



Star Formation Rate

(Kim et al. 2013)

- The SFR shows a strong primary burst caused by the rapid gas inflow to the ring due to the bar growth.
- After a few bursts, the SFR decreases rapidly since the bar region becomes almost empty due to gas inflows.
- The SFR in the nuclear ring is roughly equal to the mass inflow rate to the ring.



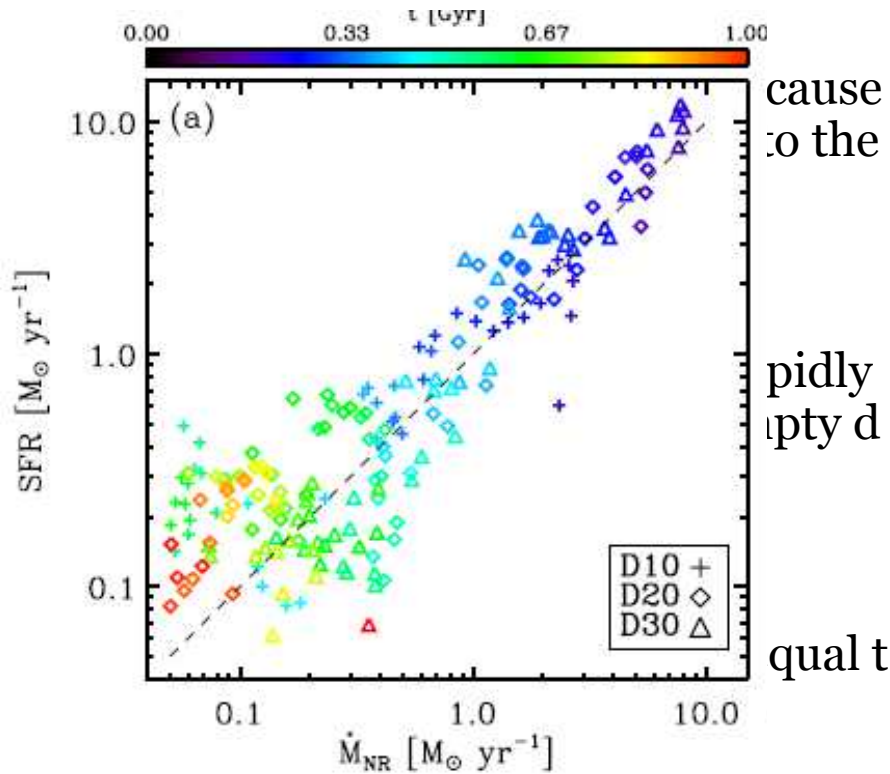
Star Formation Rate

(Kim et al. 2013)

• The
d
ba

• Af
sir
ue

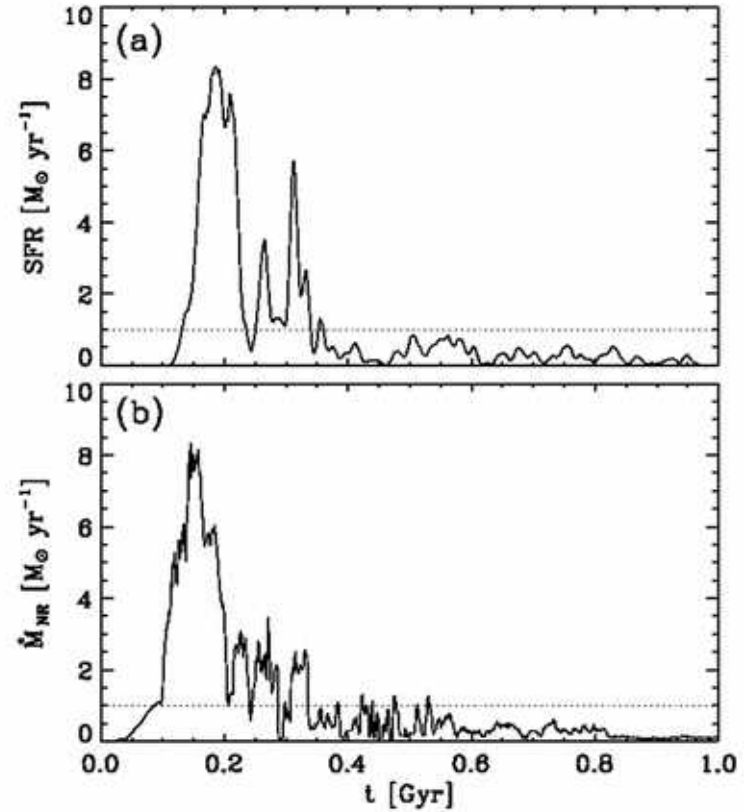
• Th
ot



cause
to the

rapidly
decreased

quality

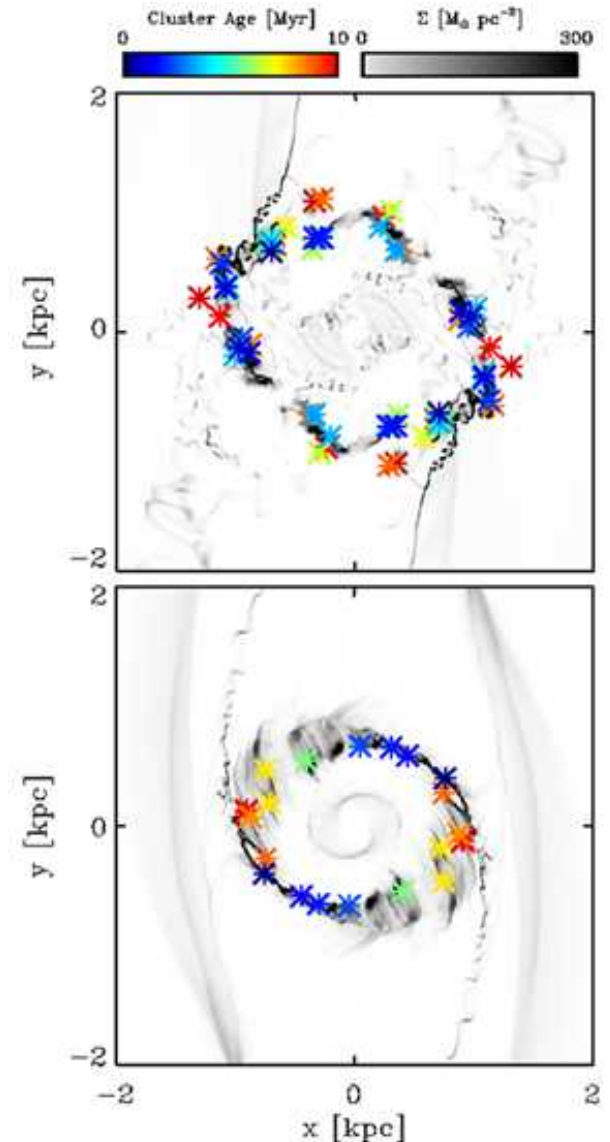


Age Gradient

(Kim et al. 2013)

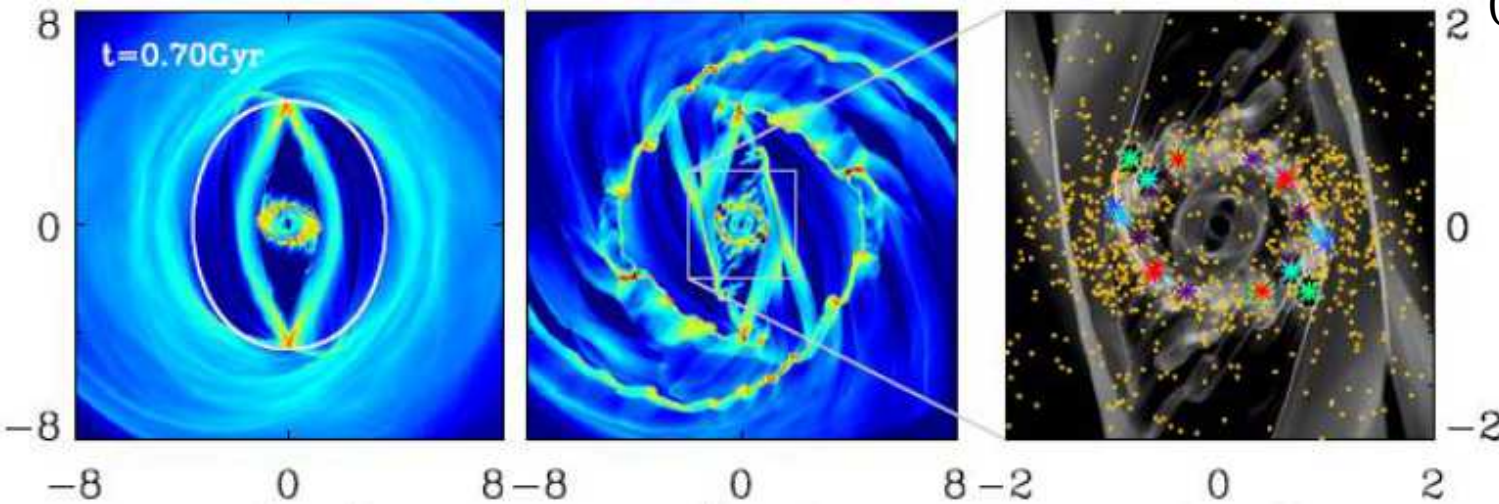
- When the SFR is larger than $1 M_{\odot} \text{ yr}^{-1}$:
 - Star formation events are widely distributed throughout the whole length of the ring.
- When the SFR is smaller than $1 M_{\odot} \text{ yr}^{-1}$:
 - Ages of young star clusters exhibit an azimuthal gradient along the ring, since star formation events take place mostly near the contact points.

$$\dot{M}_{*,\text{CP}} = \frac{2\epsilon_{\text{ff}}\Sigma_{\text{CP}}r_{\text{NR}}\Delta r\Delta\phi}{t_{\text{ff}}} \sim 1 M_{\odot}/\text{yr}$$

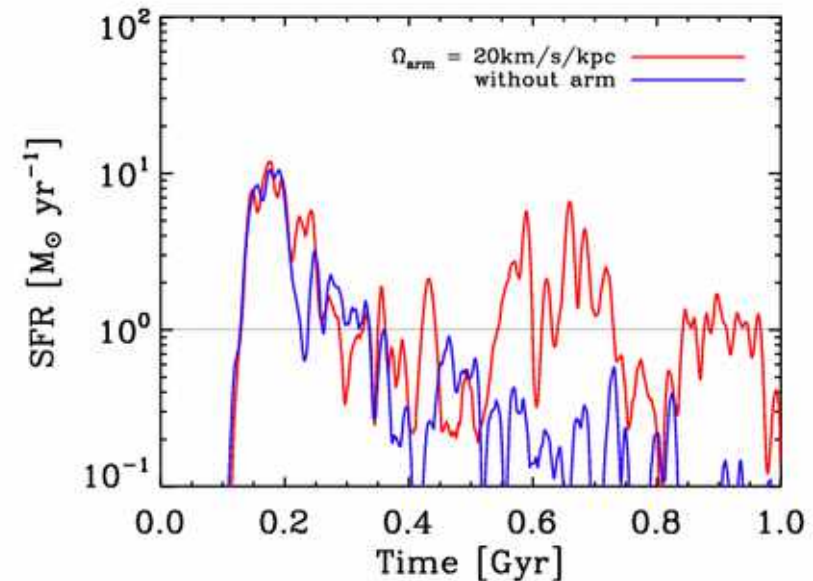


Star Formation with Spiral Arms

(Kim et al. 2014)



- Spiral arms can be efficient to transport the gas from outside to the central bar region.
- The presence of spiral arms can make the SFR rejuvenated at $t > 0.4$ Gyr.

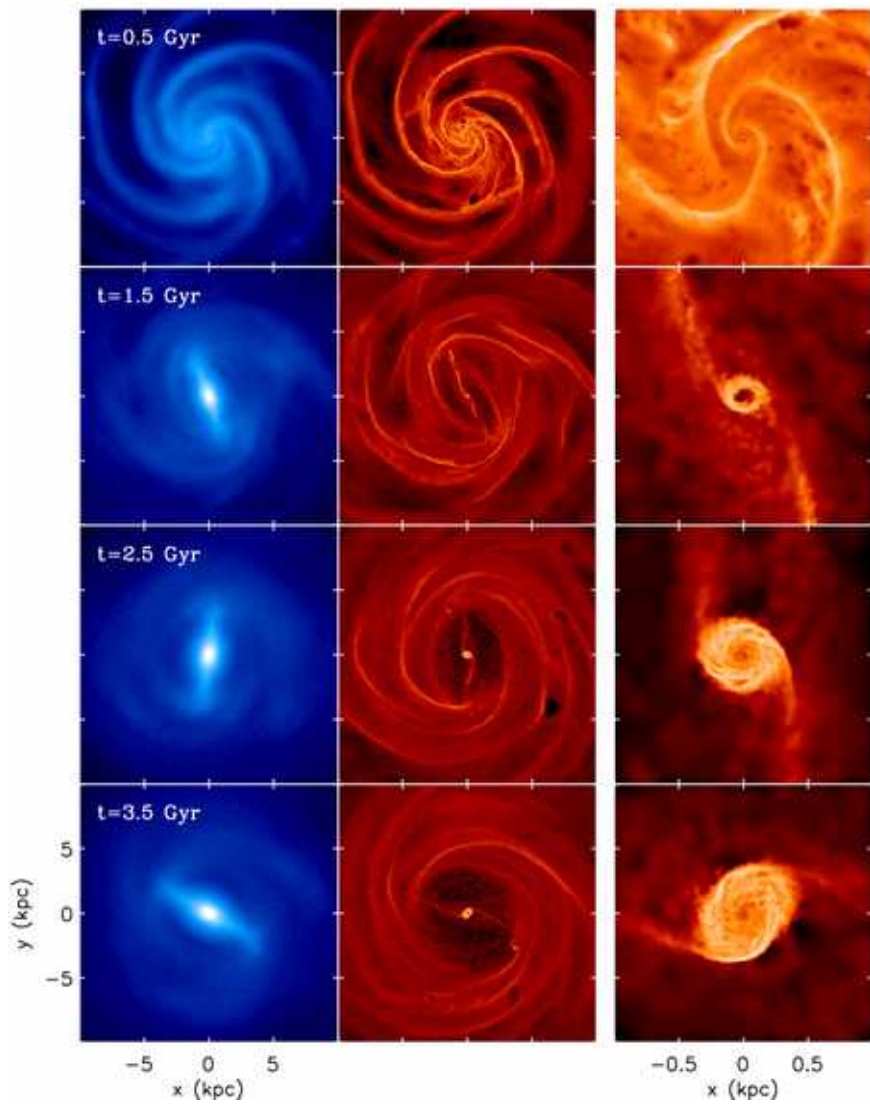


3D simulations

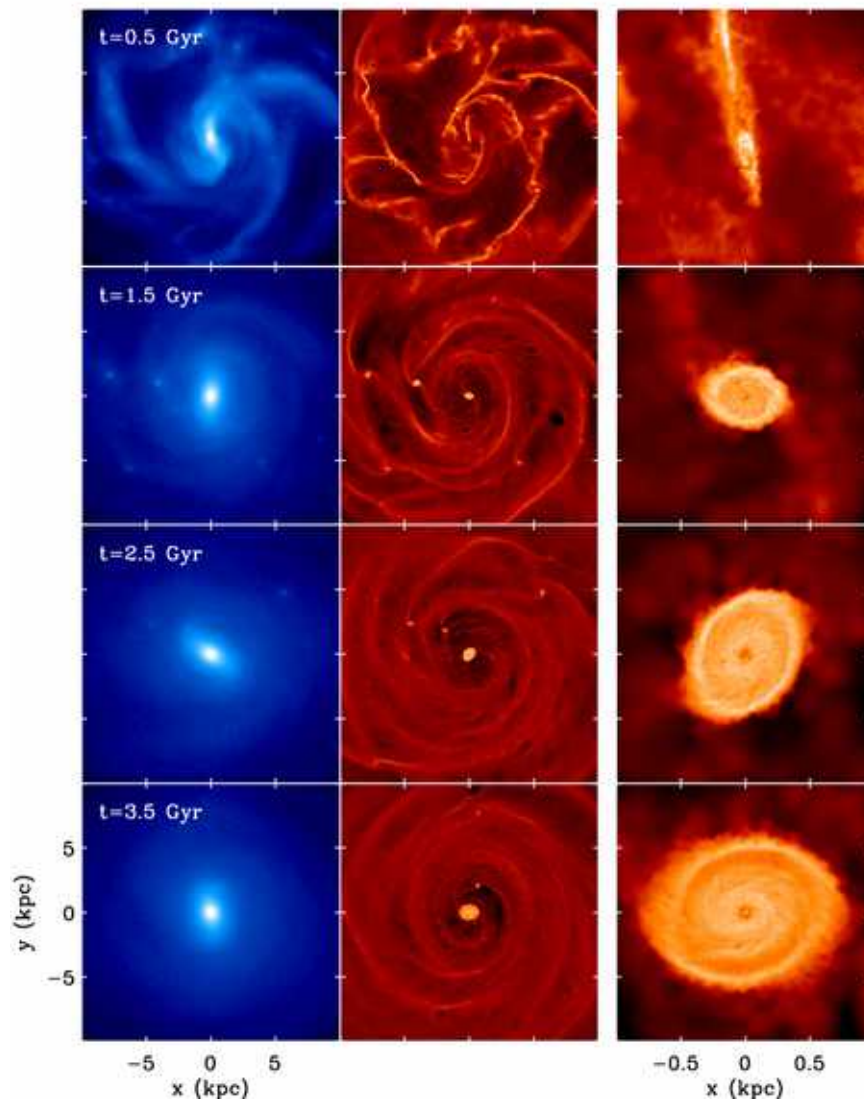
- We run fully self-consistent 3D simulations with live stellar disks and dark matters using the mesh-free hydrodynamic code GIZMO.
- The realistic star formation and feedback schemes (FIRE) include Type Ia/II supernovae, stellar winds, HII heating, etc.
- Initial conditions
 - Total disk mass : $5 \times 10^{10} M_{\odot}$
 - Disk scale length : 3 kpc
 - Vertical scale height : 300 pc
 - Gas fraction : 5, 10%
 - Gas mass inside 10 kpc $\sim 2.5, 5 \times 10^9 M_{\odot}$
(in case of 2D models $\sim 4 \times 10^9 M_{\odot}$)

Overall Evolutions

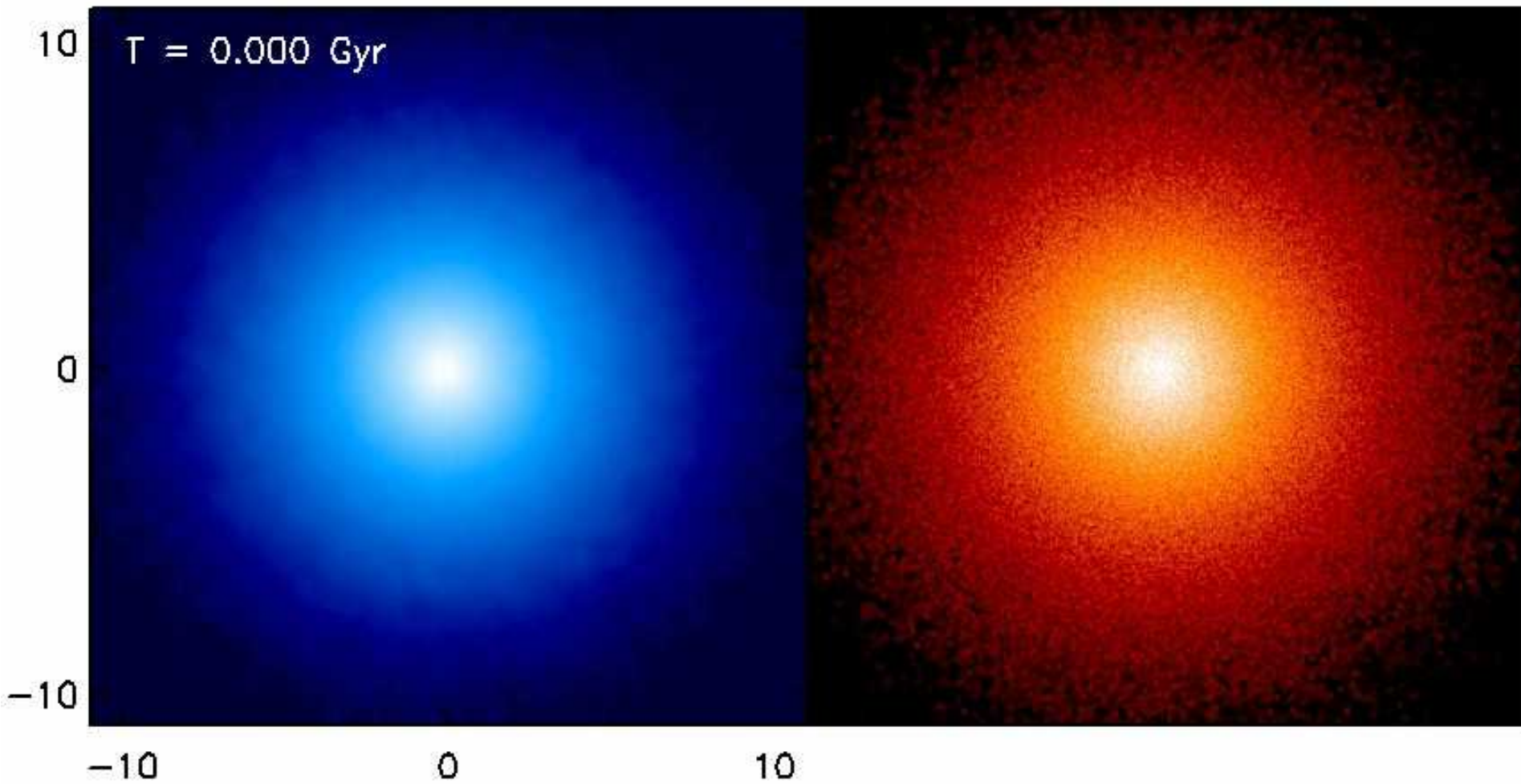
Model F05



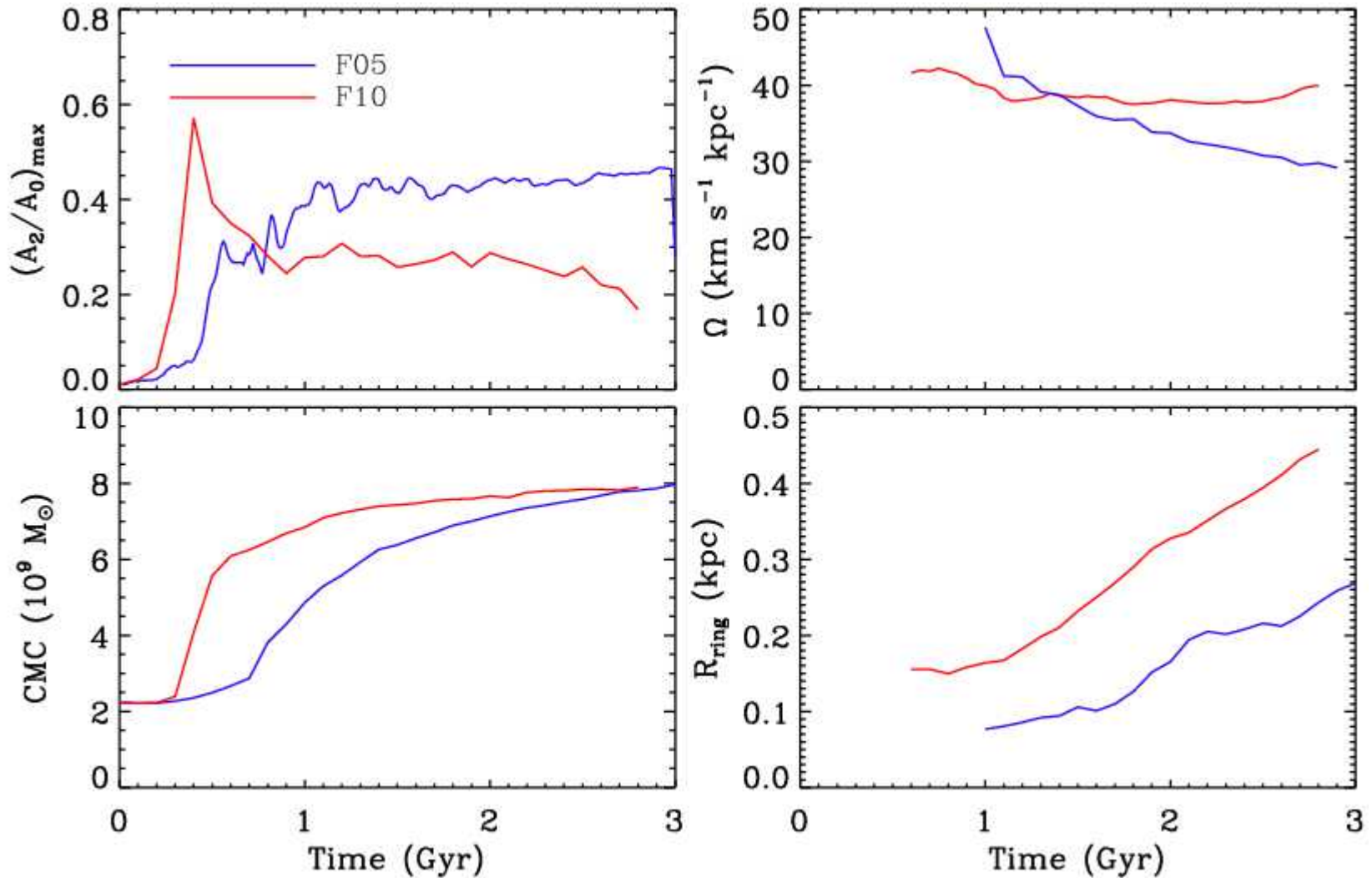
Model F10



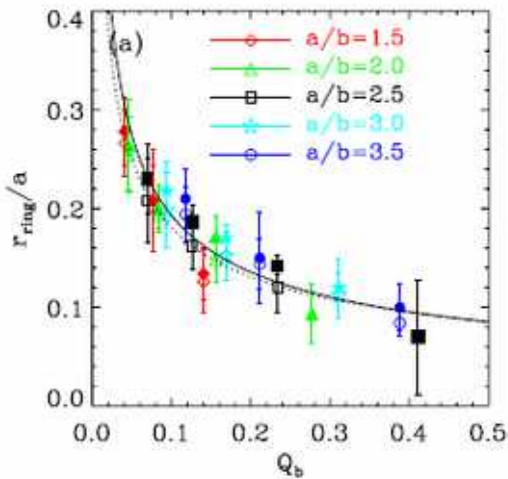
3D simulations



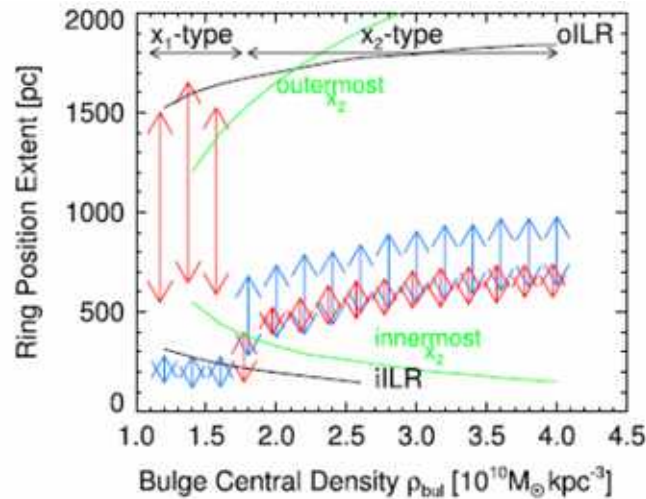
Bar Properties and Ring size



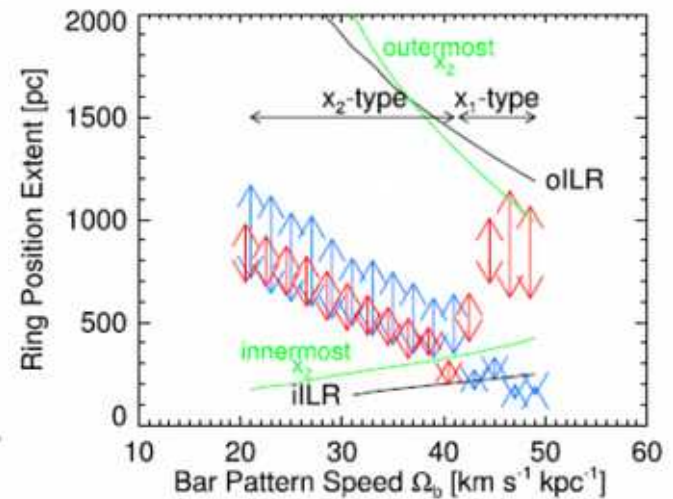
What controls size of the ring?



(Kim, Seo, Kim 2012)

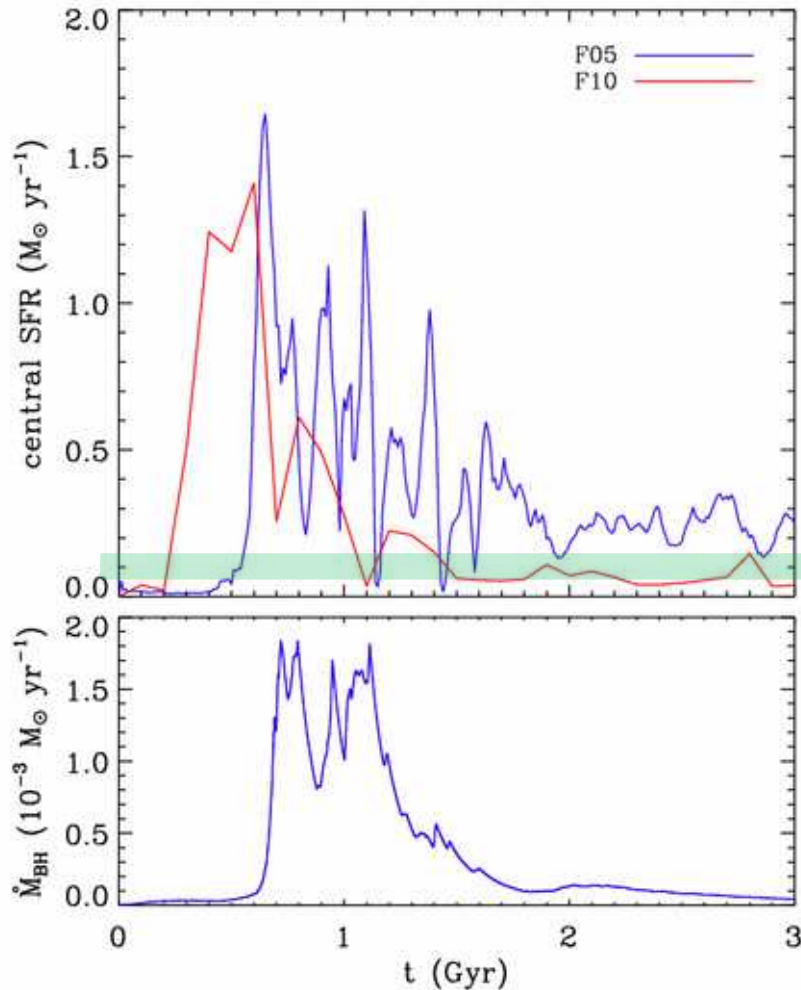


(Li, Shen, Kim 2015)



- Size of the nuclear ring increases with decreasing bar strength and pattern speed, and increasing CMC.

Star Formation in 3D Models



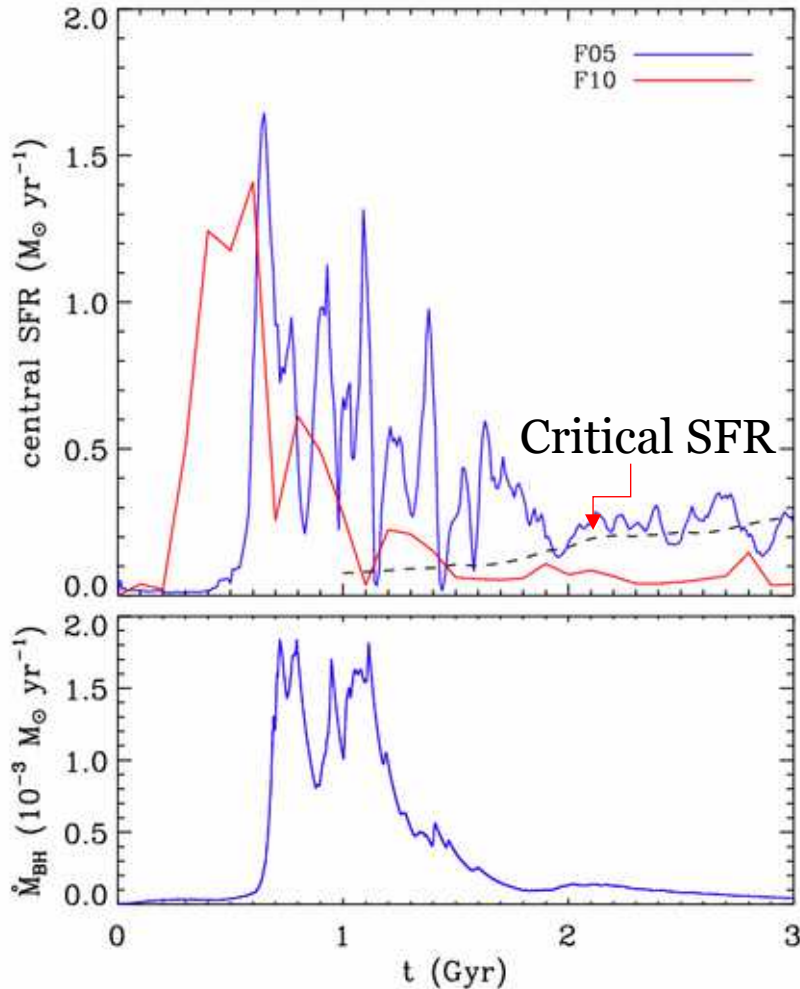
- Model F05 (Blue) :

- The phase of active star formation period is longer than the 2D Models since the bar forms more slowly.
- Several sudden drops in SFR at the stage of active star formation are due to supernovae feedback in the center.
- After the clear ring is formed, the mass inflow rate to the black hole becomes very small.

- Model F10 (Red) :

- The overall shape of the SFR is similar to that of the 2D simulations.

Star Formation in 3D Models



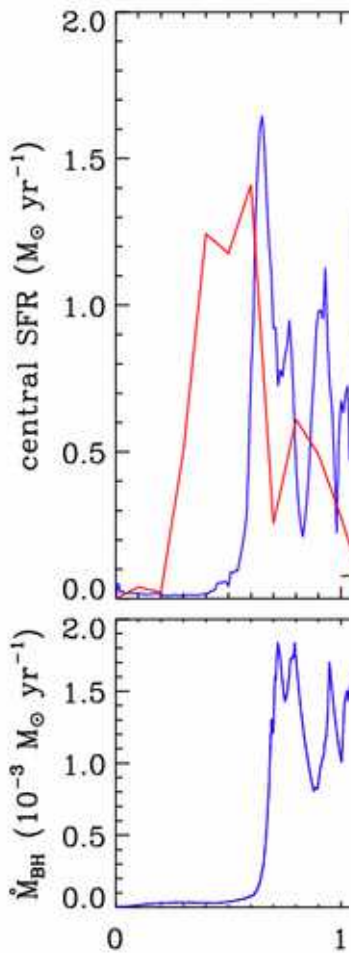
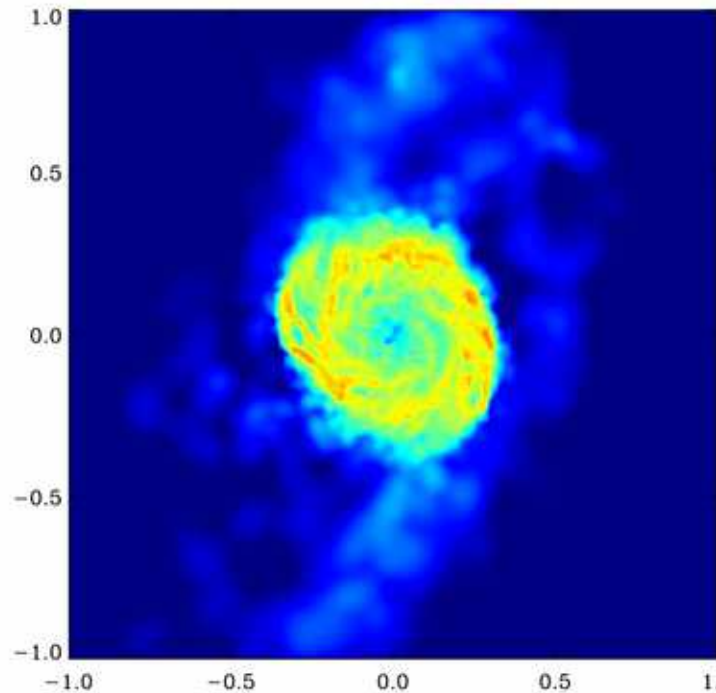
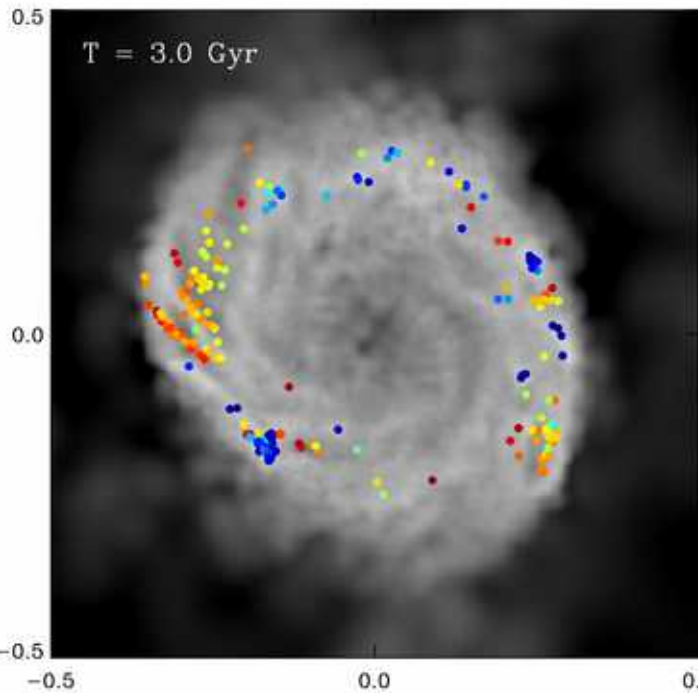
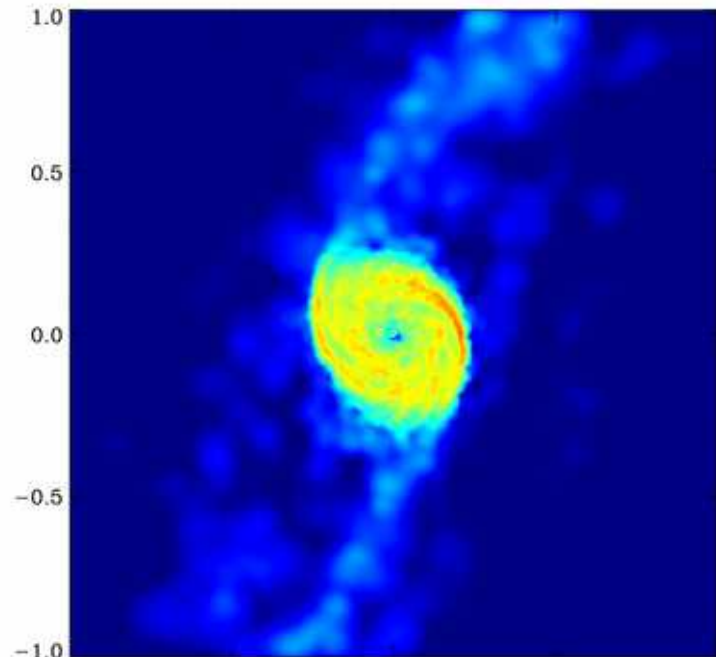
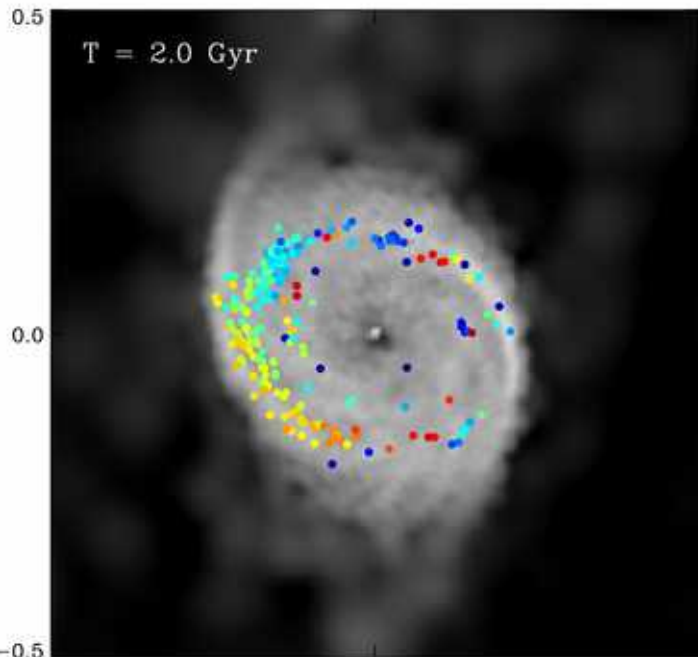
- Model F05 (Blue) :

- The phase of active star formation period is longer than the 2D Models since the bar forms more slowly.
- Several sudden drops in SFR at the stage of active star formation are due to supernovae feedback in the center.
- After the clear ring is formed, the mass inflow rate to the black hole becomes very small.

- Model F10 (Red) :

- The overall shape of the SFR is similar to that of the 2D simulations.

Star Fo



-0.5 0.0 0.5 -1.0 -0.5 0.0 0.5 1.0

Compare with Milky Way

- Physical parameters of the Milky Way
(compare with Model F05 at $t \sim 2$ Gyr)
 - Mass of molecular gas in the CMZ $\sim 2\text{-}5 \times 10^7 M_{\odot}$. ($\sim 3 \times 10^7 M_{\odot}$)
(Launhardt et al. 2002; Molinari et al. 2011)
 - The star formation rate $\sim 0.07\text{-}0.15 M_{\odot}$ /year ($\sim 0.14 M_{\odot}$ /year)
(An et al. 2011; Immer et al. 2012)
 - Half-length of the bar ~ 3.0 kpc ($\sim 4\text{-}4.5$ kpc)
 - Pattern speed of the bar $\sim 43 \pm 9$ km/s/kpc (~ 37 km/s/kpc)
 - Stellar mass in the bulge region $\sim 1.4\text{-}1.7 \times 10^{10} M_{\odot}$
 - Stellar mass of Galactic thin bar $\sim 7 \pm 1 \times 10^9 M_{\odot}$
(Bland-Hawthorn&Gerhard 2016)
(Total stellar mass inside 5 kpc $\sim 2.3 \times 10^{10} M_{\odot}$)

Summary

- We ran numerical simulations to study gaseous structures and star formation activities in the nuclear regions of barred galaxies.
- The SFR shows a few strong bursts before declining to small values.
- Only when the SFR is smaller than the critical value, the ages of young star clusters exhibit an azimuthal gradient.
- Additional gas feeding due to spiral arms can enhance the SFR at late time.
- Size of the ring slightly decreases with time in 2D simulations, whereas it increases in 3D models.